Low-temperature phase transitions and twin-domain structure of $(NH_4)_3H(SeO_4)_2$ studied by the electron paramagnetic resonance of Cu^{2+}, VO^{2+} and SeO_3^-

1991 J. Phys.: Condens. Matter 3 3795

(http://iopscience.iop.org/0953-8984/3/21/012)

J. Phys.: Condens. Matter 3 (1991) 3795–3806. Printed in the UK

Low-temperature phase transitions and twin-domain structure of $(NH_4)_3H(SeO_4)_2$ studied by the electron paramagnetic resonance of Cu^{2+}, VO^{2+} and SeO_3^-

Wu Ching-Jiun†, Yu Jiang-Tsu, Tsai Mei-Na and Lou Ssu-Hao
Institute of Physics, National Taiwan Normal University, Taipei 11718, Taiwan, Republic of China

Received 15 January 1991

Abstract. EPR of Cu^{2+}, VO^{2+}, SeO_3^-, and other paramagnetic impurities and species were used to study the low-temperature phase transitions and twin-domain structure of $(NH_4)_3H(SeO_4)_2$ crystals. The major findings are

(i) twinning in the monoclinic phases is of the merohedral type (there are three kinds of small domain related by rotations of $\pm 120°$ abut the trigonal c axis),

(ii) EPR of Cu^{2+} or SeO_3^- reveals the coexistence of the high-temperature and the low-temperature phases below the trigonal $R\bar{3}m \rightarrow$ monoclinic $A2/a$ phase transition and on further transitions, however, into the two other low-temperature monoclinic phases a single phase was again observed and

(iii) impurities and lattice point defects created by ionizing radiations were observed to influence the twinning and crystal structure of the host compound.

1. Introduction

$(NH_4)_3H(SeO_4)_2$ (TAHSe) is a member of the compounds with the general formula of $M_3H(XO_4)_2$, where $M \equiv NH_4^+$, K^+, Rb^+ and Cs^+, and $X \equiv S$ and Se. TAHSe has been reported (Gesi 1977a, b, Osaka *et al* 1979, Kishimoto *et al* 1987, Baranov *et al* 1988) to undergo the following sequence of successive phase transitions: phase I (trigonal) $\xrightarrow{332K}$ phase II (trigonal $R\bar{3}m$) $\xrightarrow{302K}$ phase III (monoclinic $A2/a$) $\xrightarrow{275K}$ phase IV (monoclinic) $\xrightarrow{181K}$ phase V (monoclonic). The IV $\rightarrow$ V phase transition is ferroelectric (Gesi 1977a). The effect of deuteration on the phase transition temperatures has been reported by Osaka *et al* (1979); the protons play no significant role in all the phase transitions except the ferroelectric transition. The ferroelastic transition at about 302 K has been studied by Kishimoto *et al* (1987); these workers have also reported the space group and the lattice constants of phase II (trigonal $R\bar{3}m$) and phase III (monoclinic $A2/a$). The structural phase transitions and proton conductivity have been reported by Baranov *et al* (1988). Kamoun *et al* (1987) investigated the phase transitions by Raman and infrared spectroscopy.

† Permanent address: Department of Mathematics and Science Education, Taiwan Provincial Hualien Teachers' College, Hualien, Taiwan 97055, Republic of China.

0953-8984/91/213795 + 12 $03.50

A detailed crystal structure of TAHSe in any of the known phases appears to be unavailable at the present time. However, the sulphate analogue, $(NH_4)_3H(SO_4)_2$ (TAHS), has shown a sequence of successive phase transitions (Gesi 1976a, b) similar to that of TAHSe. The crystal structure of the room-temperature monoclinic $A2/a$ phase of TAHS has been reported by Suzuki and Makita (1978). The phase transitions in TAHS studied by EPR of VO^{2+} and SeO_3^- has been reported by Minge and Waplak (1984). EPR studies of the phase transitions in TAHS using Cu^{2+} and Mn^{2+} as probes have been reported by Babu *et al* (1985). The twin-domain structure of TAHS has been studied by the EPR of VO^{2+} by Fujimoto and Sinha (1981). We report in this article the results of EPR studies on the phase transitions and twin-domain structure of TAHSe, using the doped Cu^{2+} and VO^{2+} ions, and the SeO_3^- radical produced by x-irradiation as probes.

2. Experimental details

Sample crystals were grown from aqueous solutions at 40 °C, by dissolving stoichiometric quantities of ammonium selenate and selenic acid in water. Elemental analysis on the nitrogen content has confirmed the composition as $(NH_4)_3H(SeO_4)_2$. The crystals obtained are in the form of thin hexagonal plates. When observed at room temperature (290 K) under polarized light, all our sample crystals have shown a mosaic pattern of small domains and, after they were heated above the monoclinic→trigonal transition temperature, the domain pattern disappeared and a conoscopic image characteristic of uniaxial crystals was observed. The twin-domain pattern that we have observed is different from that reported by Kishimoto *et al* (1987). For x-irradiation production of the SeO_3^- radical, pure TAHSe crystals were irradiated for 1 h, using a Mo target (40 kV and 20 mA).

The X-band EPR spectrometer used in this study has been described previously (Yu and Huang 1989). For rotation studies, we use an orthogonal set of reference axes of a, b^* and c axes. These axes refer to the crystal axes of the trigonal phase of TAHSe; the c axis is the trigonal axis which is perpendicular to the hexagonal crystal plates, the a axis is parallel to a side of the hexagonal plates, and the b^* axis is mutually perpendicular to the c and the a axes.

3. Results and discussion

3.1. Phase II (trigonal $R\bar{3}m$)

Figure 1 shows the resonance patterns of the doped Cu^{2+} for rotations of the magnetic field about the three reference axes, at $T = 309$ K. Only a single chemically inequivalent species of Cu^{2+} was detected, and which has shown a very anisotropic spectrum. The spectrum can be fitted by the following $S = \frac{1}{2}$ spin Hamiltonian:

$$\mathcal{H} = g_{\parallel}\beta H_z S_z + g_{\perp}\beta(H_x S_x + H_y S_y) + A_{\parallel} I_z S_z + A_{\perp}(I_x S_x + I_y S_y). \tag{1}$$

The hyperfine patterns due to the two $I = \frac{3}{2}$ isotopes of ^{63}Cu and ^{65}Cu are not resolved, and we have neglected the Cu nuclear electric quadrupole interaction in the present

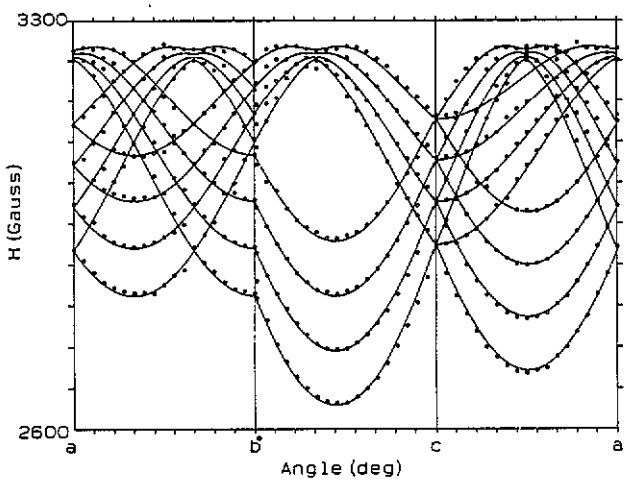

Figure 1. The observed and the fitted rotation patterns for Cu^{2+} in TAHSe at 309 K in the trigonal phase, for rotations about the three reference axes. The microwave frequency was about 9.5 GHz (in this and the other figures).

Table 1. The principal g-values and hyperfine constants for the Cu^{2+} and VO^{2+} in TAHSe.

Ion	$g_\parallel$	$g_\perp$	$A_\parallel$ (MHz)	$A_\perp$ (MHz)	T (K)
Cu^{2+}	2.438	2.091	317	17	309
Cu^{2+}	2.423	2.075	377	11	290
VO^{2+}	1.912	1.970	535	199	290
VO^{2+}	1.912	1.970	535	199	260

analysis. The resonance field is fitted by the following equation which includes second-order perturbation corrections (Abragam and Bleaney 1970):

$$H = H_0 - M(K/g\beta) - [A_\perp^2(A_\parallel^2 + A_\perp^2)/4H_0g^2\beta^2K^2][I(I+1) - M^2]$$
$$- M^2[(A_\parallel^2 - A_\perp^2)g_\parallel^2 g_\perp^2/2H_0g^5\beta^2K^2]\sin^2\theta\cos^2\theta \qquad (2)$$

where $H_0 = h\nu/g\beta$, $g^2 = g_\parallel^2\cos^2\theta + g_\perp^2\sin^2\theta$, $K^2g^2 = A_\parallel^2g_\parallel^2\cos^2\theta + A_\perp^2g_\perp^2\sin^2\theta$, and θ is the angle between the directions of the symmetry axis and the magnetic field. The spin-Hamiltonian parameters are evaluated by a least-squares fitting procedure. The evaluated parameters, which were then used to fit the observed rotation patterns shown in figure 1, are listed in table 1.

It is known that the number of possible magnetically inequivalent sites associated with a paramagnetic species is determined by the Laue symmetries of the host crystal lattice. In the trigonal $R\bar{3}m$ phase, the Laue symmetry is of the same class as the trigonal D_3 group; therefore, the number of potentially inequivalent sites is six (Yu 1988). The Cu^{2+} spectrum can be fitted by assuming that it possesses axial symmetry, with the symmetry axis lying on the b^*–c plane. Consequently, there are magnetic degeneracies for rotations of the field about the three reference axes; the number of distinguishable

magnetically inequivalent sites is three, two and three, respectively, for rotations about the c, the a and the b^* axes.

The principal g-values and hyperfine constants of the Cu^{2+} in TAHSe are comparable with those of Cu^{2+} which replaces Ca^{2+} in $Ca(OH)_2$ and $Ca(OD)_2$ (Wilson *et al* 1970, Holuj and Wilson 1973). The space group of $Ca(OH)_2$ or $Ca(OD)_2$ is the trigonal $P3(2/m)1$, which is of the same Laue symmetry class as the trigonal $R\bar{3}(2/m)1$ of TAHSe in phase II. In either $Ca(OH)_2$ or $Ca(OD)_2$, Cu^{2+} is coordinated to a distorted octahedron of oxygen atoms and, below about 145 K, Cu^{2+} is statically Jahn–Teller distorted (Wilson *et al* 1970). The principal spin-Hamiltonian parameters are, for $Ca(OH)_2$, $g_\parallel = 2.421$, $g_\perp = 2.079$, $^{65}A_\parallel = 142$ G, $^{63}A_\parallel = 132$ G and $^{63}A_\perp = {}^{65}A_\perp = 0$ G; these values are comparable with those for Cu^{2+} in TAHSe (see table 1). Thus, it can be inferred that Cu^{2+} in TAHSe is coordinated to six oxygen atoms of the selenate groups and that the Cu^{2+} is under the effect of static Jahn–Teller distortion.

TAHSe crystals turned brownish in colour after x-irradiation and an EPR spectrum which can be identified as due to the SeO_3^- radical can be detected immediately after irradiation. Figure 2 shows an $H \parallel c$ EPR spectrum of SeO_3^- in TAHSe at 160 K (a similar spectrum can be detected in the trigonal phase). In the trigonal $R\bar{3}m$ phase, the SeO_3^- radical is observed to be of axial symmetry, with the symmetry axis parallel to the trigonal c axis. Furthermore, only one SeO_3^- species is observed, which suggests that all the selenate tetrahedra in the trigonal phase are all chemically equivalent. At 301 K, the evaluated spin-Hamiltonian parameters for the SeO_3^- in TAHSe are $g_\parallel = 2.002$, $g_\perp = 2.012$, $^{77}A_\parallel = 609$ G and $^{77}A_\perp = 427$ G which are comparable with those observed for the same species in TAHS by Minge and Waplak (1984).

3.2. *Phase II → phase III transition*

Figure 3 shows a series of the $H \parallel c$ EPR spectra of Cu^{2+} in the vicinity of the phase II → phase III transition in TAHSe. The transition temperature as determined by the EPR of Cu^{2+} is about 297 K on cooling. The spectra shown in figure 3 also indicate a possible coexistence of phase II and phase III below the transition. This phenomenon is not related to the stability of the sample temperature, because it persisted even after the sample crystal had been cooled and held well below the transition temperature for some time. The coexistence of the two phases shows up most clearly and convincingly in the rotation patterns shown in figure 4. Upon comparing the rotation patterns observed at 290 K with those observed at 309 K (see figure 1), it immediately becomes clear that portions of the data points at 290 K correspond to those observed at 309 K; these portions of the rotation patterns can be fitted by using the same spin-Hamiltonian parameters evaluated at 309 K (see figure 4). The remaining portions of the rotation patterns which showed a stronger signal intensity can be identified as due to those portions of the crystal sample which had transformed into phase III. It can be noted that the general appearance of the rotation patterns related to phase III are similar to those of phase II. This can be explained by assuming that the monoclinic $A/2a$ phase (Kishimoto *et al* 1987) is twinned, and that the symmetry relations between the twin domains are the $\pm 120°$ rotations about the c axis. In fact, the patterns due to phase III can be fitted by the following assumptions.

(i) The crystal structure of the individual domains is monoclinic, and the unique twofold axis for one kind of twin domain (domain I) is parallel to the a axis of the phase II trigonal lattice (for convenience, a hexagonal crystal lattice is being used to describe the rhombohedral crystal structure).

Figure 2. The $H \| c$ EPR spectrum of the SeO_3^- radical at 160 K in phase V. The main ($I = 0$) line and the two hyperfine (^{77}Se, $I = \frac{1}{2}$) lines are each flanked by a pair of satellite lines which can be construed as arising from coupling to a nearby proton. This spectrum indicates that, in phase V, there is only one chemically inequivalent SeO_3^- species, with the implication that all the selenate tetrahedra are equivalent in this phase. A similar EPR spectrum can be observed at 301 K in phase II.

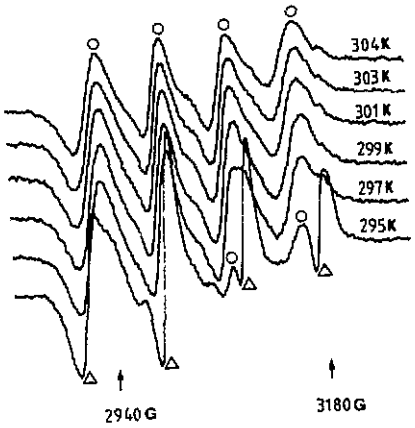

Figure 3. The $H \| c$ EPR spectra of Cu^{2+} in TAHSe at temperatures in the vicinity of the phase II → phase III transition: ○, EPR lines due to the high-temperature phase; △, EPR lines due to the low-temperature phase. A coexistence of phase II and phase III below the structural phase transition can be noted.

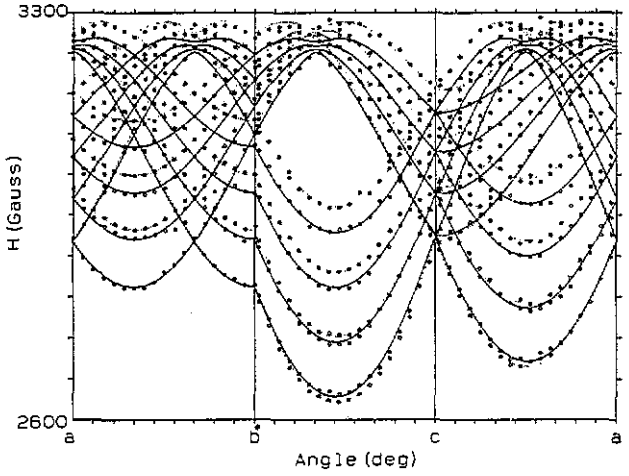

Figure 4. The observed and the fitted rotation patterns for Cu^{2+} in TAHSe at 290 K, which is below the phase II → phase III transition, showing the coexistence of the high-temperature phase and the low temperature phase most clearly in these patterns: ....., high-temperature trigonal phase; ——, low-temperature monoclinic phase. The patterns for the low-temperature monoclinic phase are of stronger EPR signal intensity than patterns for the high temperature trigonal phase. These patterns also clearly demonstrate that the weaker patterns (high-temperature trigonal phase) are not part of the resolved hyperfine patterns of the two $I = \frac{3}{2}$ natural isotopes of Cu.

(ii) The reference b^* axis is a crystal axis for domain I, and the two in-plane crystal axes of the other two kinds of twin domain are related to those of domain I by rotations of $\pm 120°$ about the c axis.

(iii) The Cu^{2+} is still of axial symmetry and the symmetry axis of domain I lies on the b^*–c plane.

Then, taken as a whole, the apparent Laue symmetry of the phase III twin domains is identical with that of the trigonal $R\bar{3}m$ phase (Yu 1988), and this explains the generally similar appearances of the rotation patterns due to phase III and phase II portions of the mixed-phase crystal sample.

In single-domain monoclinic crystals, the maximum number of magnetically inequivalent sites associated with a paramagnetic species is two. Now, in the present case, the $S = \frac{1}{2}$ species (Cu^{2+} or VO^{2+}) is of axial symmetry with the symmetry axis lying on the b^*–c plane (for domain I); then the two magnetically inequivalent sites become fully degenerate at all orientations. In other words, with the assumptions made, each type of twin domain contributes at most one set of lines to the rotation pattern of the whole crystal. For rotations about the trigonal c axis, the three kinds of domain are inequivalent, and likewise for rotations about the b^* axis; for rotations about the a axis, two kinds of twin domain (II) and (III) become degenerate, and the rotation pattern of the crystal shows two sets of lines.

To obtain information regarding the possible type of point group symmetry in phase III, we note that the unique twofold axis is a principal axis for the g-tensor and the hyperfine tensor for Cu^{2+} (and VO^{2+}). On the assumption that this has its origin in Cu^{2+} occupation site symmetry, then it can be inferred that the Cu^{2+} is located at the twofold axis or on a mirror plane perpendicular to the twofold axis. The space group of the monoclinic phase III has been reported by Kishimoto *et al* (1987) as $A2/a$, but the details of the crystal structure are still wanting. In subsequent discussion, we assume that the structure of the monoclinic $A2/a$ phase of TAHSe is similar to that of the monoclinic $A2/a$ phase of TAHS (Suzuki and Makita 1978). In this structure, the sulphate (selenate) tetrahedra are all chemically equivalent, and there are two NH_4^+ groups with different chemical environments; N(1) occupies a special position at the twofold axis, while N(2) occupies a general position. Thus, it can be assumed that Cu^{2+} preferentially occupies the N(1) site which is coordinated to a distorted octahedron of sulphate (selenate) oxygen atoms (the g-values and hyperfine constants are consistent with this; see section 3.1).

The coexistence of phase II and phase III below the phase II → phase III transition also manifests itself in the EPR spectrum of the SeO_3^- radical. Figure 5 shows a sequence of the ^{77}Se ($I = \frac{1}{2}$) hyperfine line for low fields at temperatures above and below the phase III → phase IV transition. In phase II, only one chemically inequivalent SeO_3^- radical is observed by EPR, and this indicates that the selenate tetrahedra are all chemically equivalent in the trigonal phase. On passing through the phase II → phase III transition, two chemically inequivalent SeO_3^- are observed and, upon comparing the rotation patterns with those of the trigonal phase, it becomes clear that one set of the resonance lines corresponds to that of the trigonal phase, just like the Cu^{2+} spectrum below the phase II → phase III transition. The symmetry axis for the SeO_3^- associated with the monoclinic phase departs from the trigonal c axis, reflecting the loss of trigonal symmetry below the phase transition. In phase III, the symmetry axis of SeO_3^- makes an angle of about 7° with the c axis. Since the SeO_3^- radicals related to the monoclinic $A2/a$ phase are all chemically equivalent, this implies that the selenate tetrahedra are all chemically equivalent.

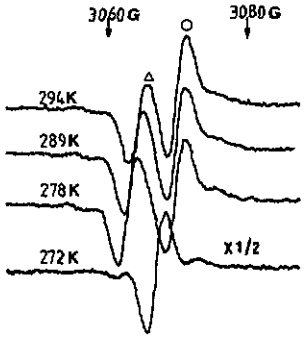

Figure 5. The $H \| c$ EPR spectra of the ^{77}Se hyperfine line for low fields at temperatures above and below the phase III → phase IV transition. In phase III, there are two chemically inequivalent SeO_3^-; one (○) shows rotation patterns identical with the SeO_3^- in the trigonal phase. The SeO_3^- associated with the monoclinic, phase III is also shown (△). It can be noted that below the phase III → phase IV transition, only one SeO_3^- is observed, indicating that the crystal sample is again of a single phase in phase IV.

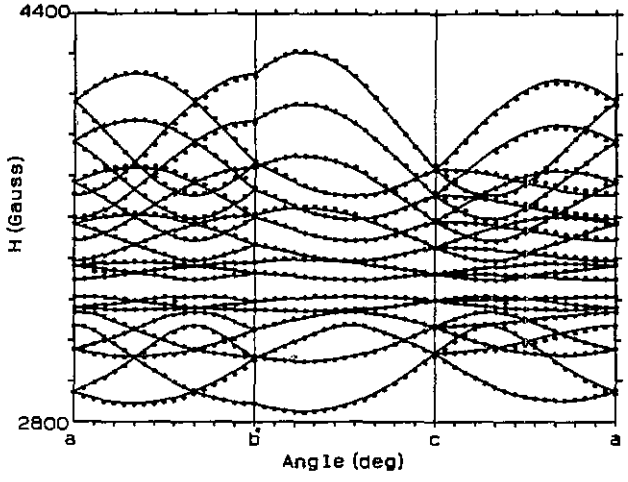

Figure 6. The observed and the fitted rotation patterns for VO^{2+} in TAHSe at 290 K in phase III.

Figure 6 shows the rotation patterns of VO^{2+} at 290 K, which is below the phase II → phase III transition. It can be noted that the general appearance of the observed patterns are similar to those of Cu^{2+} at the same temperature, except that there is only one chemically inequivalent species of VO^{2+}. This implies that TAHSe doped with VO^{2+} is of a single phase below the phase II → phase III transition (this phenomenon will be further discussed later). The VO^{2+} rotation patterns shown in figure 6 are similar in appearance to those observed in the trigonal phase (not shown), and this may be susceptible to the explanation that the host crystal lattice remains trigonal. However, VO^{2+}-doped TAHSe crystals at room temperature show a mosaic pattern of small domains, similar to those of the pure and Cu^{2+}-doped TAHSe crystals and, upon heating above the phase III → phase II transition, the crystals become single domains and display a conoscopic image characteristic of uniaxial crystals. Therefore, we assume that VO^{2+}-doped TAHSe crystals in phase III are of the twinned monoclinic structure.

The VO^{2+} rotation patterns shown in figure 6 can be fitted in a manner similar to those for Cu^{2+}; that is the $S = \frac{1}{2}$ species of VO^{2+} can be assumed to be of axial symmetry, with the symmetry axis lying on the b^*–c plane (for domain I). The evaluated spin-Hamiltonian parameters are listed in table 1, and the fitted patterns are plotted in figure

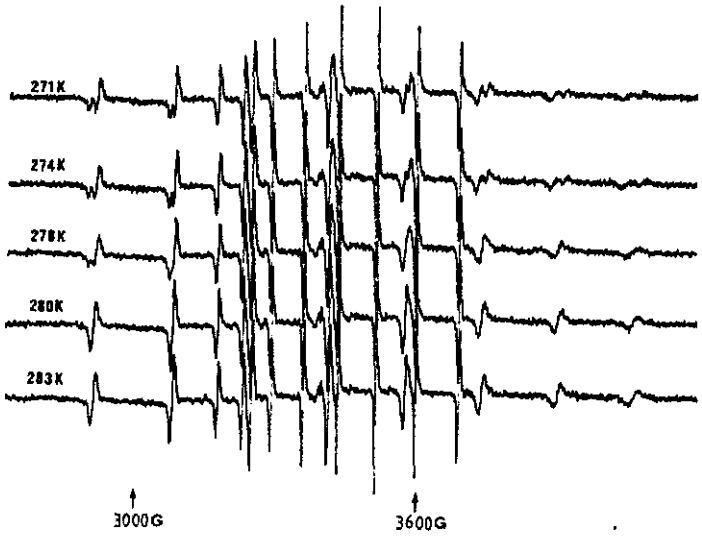

Figure 7. The $H \| a$ EPR spectra of VO^{2+} at temperatures below and above the phase IV → phase III transition. Upon transition to phase IV, the VO^{2+} is split into two chemically inequivalent species with identical principal g-values and hyperfine constants but different orientations of the symmetry axis.

6. It can be noted that the unique twofold axis of the monoclinic $A2/a$ phase is a principal axis for the **g**-tensor and the hyperfine tensor for VO^{2+}, and this implies a preferential occupation of VO^{2+} at the N(1) site.

3.3. Phase III → phase IV transition

As can be noted from the $H \| c$ spectrum shown in figure 5, only one chemically inequivalent species of SeO_3^- can be detected below the phase III → phase IV transition (the transition temperature is about 279 K on cooling). This implies that the x-irradiated sample crystal is again of a single phase, and that the selenate tetrahedra are still chemically equivalent in phase IV.

Figure 7 shows a sequence of the $H \| a$ spectra of VO^{2+} at temperatures below and above the phase IV → phase III transition (the transition temperature is about 280 K on heating). The observed and the fitted rotation patterns at 260 K are shown in figure 8, which indicates the presence of two chemically inequivalent VO^{2+} species (denoted as species 1 and 2) in phase IV. The rotation patterns of either $(VO^{2+})_1$ or $(VO^{2+})_2$ can be fitted by assuming that they are still of axial symmetry, and that the symmetry axis lies on the b^*–c plane (for domain I). The evaluated principal g-values and hyperfine constants (see table 1) are identical for these two species, but the symmetry axis of $(VO^{2+})_1$ (full curves in figure 8) makes an angle of 70° with the c axis, whereas this angle is 66° for $(VO^{2+})_2$ (dotted curves in figure 8). For comparison, this angle is 66° in phase III. This phenomenon, namely having two VO^{2+} species with identical principal g-values and hyperfine constants but different orientations of the principal axis, has also been reported for the VO^{2+} in the monoclinic $A2/a$ phase of TAHS (Minge and Waplak 1984, Fujimoto and Sinha 1981). This has been explained by these workers as due to a strain-induced splitting in the ferroelastic phase.

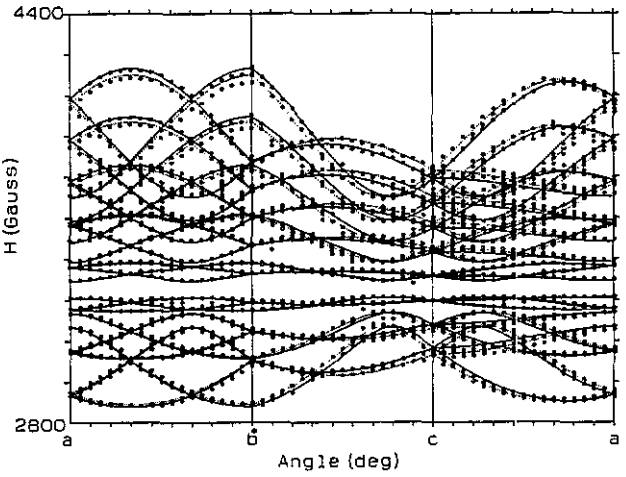

Figure 8. The observed and the fitted rotation patterns at 260 K for the two chemically inequivalent species of $(VO^{2+})_1$ and $(VO^{2+})_2$ (.....) in phase IV.

3.4. *Phase IV → phase V transition*

The phase IV → phase V ferroelectric transition has been reported (Osaka *et al* 1979) to be the only transition in TAHSe in which hydrogen bonds of the O—H···O type play a significant role. Figure 9 shows a sequence of the hyperfine line of SeO_3^- for low fields, at temperatures above and below the reported transition at about 181 K. It can be noted that the spectra do not show any anomalous change in either resonance field or linewidth on passing through the reported transition temperature. The same can be said for the EPR of the Cu^{2+} and VO^{2+} in TAHSe. We have also found that the EPR of the Fe^{3+} used for doping TAHSe crystals, although sensitive to the other reported phase transitions, is insensitive to the transition at 181 K. The results presented above suggest that the doped Cu^{2+} or VO^{2+} occupies the N(1) site in TAHSe; therefore, an NH_4^+ vacancy or an acid-proton vacancy would be created which could be local or non-local to the doped paramagnetic impurity. If the charge-compensating vacancy is of the acid-proton type and local to the doped impurity, then the EPR of either Cu^{2+} or VO^{2+} may be insensitive to the ferroelectric phase transition. In TAHSe, the selenate oxygen atoms should be hydrogen bonded to the acid protons, and the creation of the SeO_3^- radical by x-irradiation would result in the breaking of the hydrogen bonds, and this may explain the insensitivity of the EPR of SeO_3^- to the ferroelectric transition which has been reported to be dominated by the motion of the acid protons.

3.5. *Effects of impurities and lattice point defects on the crystal structure and twinning in TAHSe*

We have found a rather unique property of the TAHSe crystals: the crystal structure and twinning can be observed to be influenced by impurities or lattice point defects created by x-irradiation. We have grown TAHSe crystals doped with Mn^{2+} from aqueous solutions held at 40 °C, and the crystals obtained were in the form of thin hexagonal plates which show a mosaic pattern of small domains when viewed in polarized light. Upon heating above the monoclinic → trigonal transition temperature, the domain pattern disappears

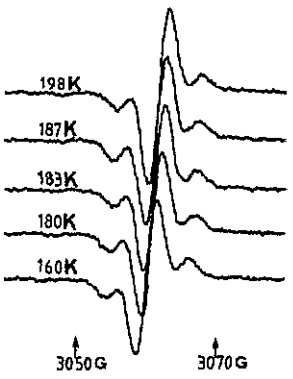

Figure 9. The $H \| c$ EPR spectra of the ^{77}Se hyperfine line for low fields at temperatures above and below the reported ferroelectric transition at about 181 K. The spectrum of SeO_3^- shows a continuous change on passing through this transition, without showing any anomaly in either spectrum or linewidth.

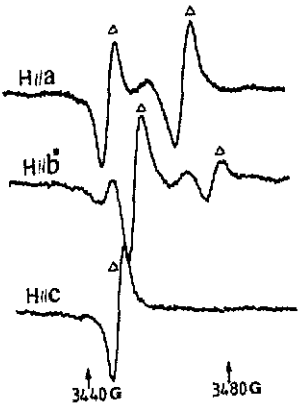

Figure 10. The room-temperature EPR spectra, at the three reference axes for TAHSe, observed for the γ-ray-produced CrO_4^{3-} radical (Δ). It can be noted that this radical does not show any proton hyperfine coupling in this hydrogen-bonded compound.

and displays a uniaxial interference figure, just like pure and Cu^{2+}- or VO^{2+}-doped TAHSe crystals. Such Mn^{2+}-doped crystals show six hyperfine lines of ^{55}Mn at room temperature (monoclinic $A2/a$ phase). However, when grown at 20 °C, the Mn^{2+}-doped TAHSe crystals are of single domains and show a conoscopic image characteristic of biaxial crystals. On heating above the reported monoclinic → trigonal transition temperature, the crystals remain biaxial; the reported monoclinic → trigonal transition is not observed. Such crystals display a very broad EPR line centred at $g \simeq 2$, similar to that of Mn^{2+} in TAHS reported by Minge and Waplak (1984). It is known that an H_2O inclusion (in the form of a transition-ion complex) is more likely to occur in crystals grown at lower temperatures than in those grown at higher temperatures; the differences between the crystal structure and twinning observed in the two types of Mn-doped TAHSe crystal could be related to the formation of the Mn^{2+}–H_2O complex.

We have grown TAHSe crystals doped with CrO_4^{2-} which shows the yellow colour characteristic of the CrO_4^{2-} ion. CrO_4^{2-}-doped crystals have single domains and show at room temperature a conoscopic image typical of uniaxial crystals. Chemical analysis has confirmed the composition as $(NH_4)_3H(SeO_4)_2$ and x-ray diffraction has confirmed the structure as trigonal $R\bar{3}m$ (Kishimoto *et al* 1987). Thus, doping with CrO_4^{2-} appears to stabilize the trigonal $R\bar{3}m$ phase. When irradiated with γ-rays (for a total dosage of about 5 MRad), CrO_4^{2-}-doped TAHSe crystals show an EPR spectrum at room temperature which can be identified as due to the CrO_4^{3-} radical (figure 10). The rotation patterns of this CrO_4^{3-} are similar in appearance to those of Cu^{2+} or VO^{2+}; the principal g-values are 1.947, 1.967 and 1.971, indicating that the odd electron is localized principally in the $3d_{x^2-y^2}$ orbital. Furthermore, the EPR of the γ-ray-produced CrO_4^{3-} is insensitive to the sequence of low-temperature phase transitions in TAHSe. Unlike the situation in other hydrogen-bonded compounds, the CrO_4^{3-} radical (which is expected to occupy the selenate site) in TAHSe does not show any hyperfine coupling to nearby protons (see figure 10), and this may be explained by the breaking of the local hydrogen bonds by the

γ-ray photons. The CrO_4^{2-}-doped TAHSe crystals, when heated to temperatures above about 100 °C, show an EPR spectrum identical with that produced by γ-irradiation. This thermally produced CrO_4^{3-} radical is also insensitive to the low-temperature phase transitions. Heating at high temperatures could result in the molecular dissociation of the NH_4^+ group (which we believe is the origin of the unpaired electron acquired by the doped CrO_4^{2-} to form the paramagnetic CrO_4^{3-}) and the breaking of the local hydrogen bonds, and this may be the reason why the CrO_4^{3-} radical produced either by γ-irradiation or by thermal heating is insensitive to the low-temperature phase transitions.

The above results tend to indicate that impurities or lattice point defects can affect in a significant way the twinning and crystal structure of TAHSe; this unique phenomenon is worthy of further investigations.

4. Conclusions

The major conclusions regarding the crystal structure and twinning of $(NH_4)_3H(SeO_4)_2$, as revealed by the EPR of Cu^{2+}, VO^{2+} and SeO_3^- and other paramagnetic species can be summarized as follows.

(i) Twinning in the monoclinic phases of TAHSe is of the merohedral type. Three kinds of twin domain exist. One kind of twin domain (domain I) has its unique twofold axis aligned parallel to the a axis (referred to the underlying hexagonal lattice) of the high-temperature trigonal phase; the twofold axes of the other two kinds of twin domain are related to that of domain I by rotations of $\pm 120°$ about the trigonal c axis. Because the point group of the low-temperature monoclinic $A2/a$ phase is a subgroup of that of the high-temperature trigonal $R\bar{3}(2/m)1$ phase, the symmetry operations relating to the twin domains formed below the trigonal $\rightarrow$ monoclinic transition correspond to the symmetries ($\pm 120°$ rotations about the c axis) lost during the transition. Consequently, the apparent Laue symmetry of a twinned TAHSe crystal in the monoclonic phases is identical with that of the high-temperature trigonal phase.

(ii) The EPR of Cu^{2+} and SeO_3^- indicates that below the trigonal $R\bar{3}m \rightarrow$ monoclinic $A2/a$ transition, a TAHSe crystal has mixed phases: the coexistence of the high-temperature trigonal phase and the low-temperature monoclinic phase. The SeO_3^- result is particularly important in view of the fact that this radical will be continuously created (and, in particular, the implied creation of the acid-proton vacancies) during the data-collecting process in x-ray diffraction studies of the crystal structure of TAHSe.

(iii) Impurities and lattice point defects appear to influence significantly the crystal structure and twinning of TAHSe.

Acknowledgments

The authors thank Dr R H Chen for the x-irradiation of the sample crystals, and the support given by the National Science Council of the Republic of China during the period of this research.

References

Abragam A and Bleaney B 1970 *Electron Paramagnetic Resonance of Transition Ions* (New York: Dover) p 175

Babu D S, Sastry G S, Sastry M D and Dalvi A G I 1985. *J. Phys. C: Solid State Phys.* **18** 6111–9
Baranov A I, Treguchenko A V, Shuvalov L A and Shchagina N M 1988 *Sov. Phys.–Solid State* **29** 1448–9
Fujimoto M and Sinha B V 1981 *Ferroelectrics* **39**1029–32
Gesi K 1976a *Phys. Status Solidi* a **33** 479–82
—— 1976b *J. Phys. Soc. Japan* **41** 1437–8
—— 1977a *J. Phys. Soc. Japan* **42** 1785–6
—— 1977b *J. Phys. Soc. Japan* **43** 1949–53
Holuj F and Wilson R G 1973 *Phys. Rev.* B 7 4065–72
Kamoun M, Halouani M and Daoud A 1987 *Phase Trans.* **9** 327–35
Kishimoto T, Osaka T, Kamukae M and Mikata Y 1987 *J. Phys. Soc. Japan* **56** 2070–9
Minge J and Waplak S 1984 *Phys. Status Solidi* b **123** 27–36
Osaka T, Makita Y and Gesi K 1979 *J. Phys. Soc. Japan* **46** 577–80
Suzuki S and Makita Y 1978 *Acta Crystallogr.* B **34** 732–5
Wilson R G, Holuj F and Hedgecock N E 1970 *Phys. Rev.* B **1** 3609–13
Yu J T 1988 *J. Phys. C: Solid State Phys.* **21** 2103–12
Yu J T and Huang Y S 1989 *Phys. Rev.* B **40** 4281–8